

Response Surface Methodology Application in Optimization of Oily Wastewater Treatment by *Sargassum latifolium*

Walaa M. Thabet^{1*}, Ahmed E. Alprol¹, Mohamed Ashour¹, Mohamed Khedawy¹,
Esraa Aziz El-Masry²

¹National Institute of Oceanography and Fisheries (NIOF), Marine Environment Division, Cairo, Egypt

²Oceanography Department, Faculty of Science, Alexandria University, Alexandria, Egypt

* Corresponding author: thabetniof@yahoo.com

ARTICLE INFO

Article History:

Received: Jan. 19, 2024

Accepted: Feb. 12, 2024

Online: Feb. 20, 2024

Keywords:

Oily wastewater,
Treatment, Adsorbents,
Response surface
methodology,
Box–Behnken design,
Advanced treatment
technology,
Sargassum latifolium

ABSTRACT

Response surface methodology (RSM) and Box–Behnken (BB) statistical experiment design were developed to study the optimization of oily wastewater treatment using *Sargassum latifolium*. The characterization of the *Sargassum latifolium* was studied using fourier transform infrared spectroscopy (FTIR), scanning electron microscope (SEM), N₂ adsorption/desorption, and Raman techniques. These studies demonstrated the importance of various functional groups such as carbonyl, amino, carboxyl, and hydroxyl on adsorption mechanism. The specific surface area of *S. latifolium* was 111.65m²/g. Scanning electron microscope (SEM) showed that the interaction of *S. latifolium* with oil led to the development of flake-like deposits on its surface, causing the surface to become uneven. Four process-independent parameters, including contact time, oil volume, adsorbent dosage, and pH were optimized for the best response of crude oil adsorption using Box–Behnken design. The output was summarized for an additional ANOVA analysis. Optimization conditions for crude oil adsorption onto *Sargassum Latifolium* were found to be at an adsorbent dose of 0.13g, oil volume of 24.29ml, time of 57.44 minutes, and initial pH of 9.54. Langmuir and Freundlich isotherm models were used to apply equilibrium analysis. The results suggest that the Langmuir model better fits the experimental data compared to the Freundlich model. The experimental results showed that the crude oil adsorption capacity onto *Sargassum latifolium* was 45.87gm under ideal conditions, which was somewhat lower than the RSM model's value of 46.14gm.

INTRODUCTION

The most obvious and serious type of maritime contamination is oil pollution. Tankers have been spilling thousands of tons of oil per year during the past ten years (Abdelwahab *et al.*, 2021; Moneer *et al.*, 2023). Several industries, including those in the pharmaceutical, petrochemical, oil and gas, and food sectors, have added to the massive output of oil effluent globally (Abuhasel *et al.*, 2021). Oily wastewater is classified as carcinogenic, and it can contaminate drinking water and groundwater resources, as well as produce environmental imbalances and harm to human health

(Putatunda *et al.*, 2019). Traditional treatments for oily wastewater treatment include sedimentation, chemical coagulation, flotation, and gravity separation among other ways. The disadvantages of these techniques are the discharge of secondary pollutants, high operational costs, and low efficiency removal (Han *et al.*, 2019). Oily wastewater treatment can be accomplished with advanced technologies; the removal of harmful contaminants from oily wastewater using these technologies is efficient, sustainable, affordable, and environmentally benign, among other benefits (Medeiros *et al.*, 2022). Microbial bioremediation technology, batch biodegradation using a single or consortium of microorganisms, bioreactor technology, membrane technology, electrochemical technology, advanced oxidation processes (AOPs), adsorption treatment technology, and combined treatment technologies are the most famous advanced technologies for oily wastewater treatment (Adetunji & Olaniran, 2021).

Adsorption treatment technology is considered to be one of the most popular techniques for treating industrial wastewater for its efficiency in terms of industrial applicability, cost, and time for extracting dissolved oil from water (Diraki *et al.*, 2022; Alprol *et al.*, 2023). Nowadays, adsorption research for wastewater treatment is still being developed, and researchers are working to develop raw materials that will be used in the future. Finding novel materials for wastewater treatment is thus one of the most exciting research goals. For oily wastewater treatment, the most commonly used adsorbents are chitosan, palm fibers, zeolite, diatomite, bentonite, natural soil, and biosorbents such as raw barley straw. Algae have recently been used as promising biosorbents for their great potential in the removal of different pollutants for their high biosorption capacity, distinct properties, and renewable availability (Lee *et al.*, 2022; O. Abdelwahab & Thabet 2023).

Statistically constructed experiments are chosen for error reduction, parameter analysis, and low-cost data acquisition. In general, the one-variable at a time (OVAT) method is not challenging, however it has a limited ability to accurately predict the effects of interacting factors and may cause misinterpretation of the outcomes (Abd El-Hamid, AlProl & Hafiz, 2022; Soliman *et al.*, 2022). There are a variety of optimization and modeling methodologies available, starting with the simple one factorial at a time (OFAT) model and progressing to composite and nexus statistical designs such as response surface methodology (RSM) (Abd El-Hamid, AlProl & Hafiz, 2022). RSM is a statistical method for enhancing responses that are prejudiced by a number of variables (Demirel *et al.*, 2022). This optimization technique entails developing a collection of mathematical tools to aid in the creation, development, and improvement of the model.

Brown macroalgae (seaweed) called Sargassum species are found in shallow marine meadows in tropical and subtropical regions (Al Prol, El-Metwally & Amer 2019). In addition to other bioactive ingredients, these are a good source of minerals carotenoids, vitamins, proteins, and dietary fibers. In addition, several Sargassum species have been shown to contain a variety of biologically active compounds, comprising

pheophytins, sterols, terpenoids, sulfated polysaccharides, sargaquinoic acids, flavonoids, polyphenols, sargaquinoic acids, sargachromenol, and pheophytin (Ale, Mikkelsen & Meyer, 2011; Gomaa *et al.*, 2018). There is no published data on the removal of oil on the adsorbent form of *S. Latifolium* from an aqueous solution by response surface methodology modeling. Therefore, in the present study, RSM was utilized for oil removal from an aqueous solution using *Sargassum latifolium*.

MATERIALS AND METHODS

1. Adsorbent preparation

Samples of brown seaweed, *S. latifolium*, were taken in May 2022 from the intertidal zone in Suez Bay, Red Sea, Egypt, and used as an adsorbent. In situ, samples were cleaned with seawater to remove undesirable components like salts and particles that stuck to the surface. After being transported to the lab, they were cleaned with running tap water and then deionized water. *S. latifolium* was sun-dried after cleaning, and the biomass that resulted was ground into a powder using a grinder then sieved, and kept in plastic bags until needed again. One gram of powdered *S. latifolium* was soaked in 100ml of deionized water. Moreover, it was cut-milled with a 200 μ m screen size.

1.1. Characterization of adsorbents

SEM was used to perform morphological characterization (before and after the adsorption) of *S. Latifolium* (JEOL JSM 6360, Peabody, MA, USA). The impact of the produced polymeric materials was measured using FTIR and Senterra Raman spectrometer (Bruker, Billerica, MA, USA), and Raman spectroscopy on a Shimadzu FTIR-8400 S (Kyoto, Japan), respectively.

The mean pore diameter, total pore volume, and total surface area of the adsorbent were investigated by Brunauer Emmett Teller (BET). Using inert gases and a pressure environment, the pore size distribution and the adsorption-desorption isotherm were visualized. The BET analysis was carried out using the NLDFT model. The analysis was performed at 33.5ATM using inert nitrogen at 77K, gas at 87K and a 13.3Pa pressure transducer.

2.2. Adsorption experiments

A certain amount of oil was added in a 100ml of synthetic sea water. Batch experiments were carried out for oil removal. *S. latifolium* seaweed was gently and evenly placed onto the net at the oil/water interface for a certain period of time. (Abdelwahab, Nasr & Thabet, 2017) Serial volumes of oil (5, 10, 15, 20, 25ml) were mixed with doses series of adsorbent (0.1– 1g) at different pH ranges (1, 3, 7, 9, and 11) and different time intervals (10, 20, 30, 60, 90 and 120min) at room temperature. The net was used to move the fibers vertically, and then it was hung over the cell to allow the cell to drain. The weight of the sample was established and recorded, and every experiment

was conducted at room temperature. The following equation was used to compute the sorption capacity (Abdelwahab, Nasr & Thabet, 2017).
Adsorption capacity (g/g) = mass of oil removed / mass of absorbent

3. Box–Behnken experimental design

RSM and the BB design were used to evaluate the effects of the four independent variables on the response function. The independent variables were adsorbent dose (X_1), oil volume (X_2), time (X_3), and pH (X_4). Each variable's low, center and high levels are designated as -1, 0, and +1, respectively, as illustrated in Table (1). The results from preliminary experiments have been used to determine each variable experimental levels. The response function was crude oil adsorption capacity on *S. latifolium*.

Table 1. Independent variable and their levels used for BB design

Variable (Factor)/ unit	Code	Level		
		-1	0	+1
Adsorbent dose (gm)	X_1	0.2	0.6	1
Oil Volume (ml)	X_2	5	15	25
Time (min)	X_3	10	30	120
pH	X_4	6	9	11

The preliminary equations for the Box-Behnken experimental design that were applied in this study are shown in Table (1). Equations 2 and 3 were used to code the variables and determine how many experiments were necessary to produce the Box-Behnken to assess the impact of the four primary independent parameters on the effectiveness of oil adsorption, a total of 29 trials have been used in this study. Equation 4 describes the input process parameters and the response relationship. The response (y), which depends on the input factors X_1, X_2, \dots, X_k , was analyzed to assess the process's performance. Either in three dimensions or as contour plots that exhibit the contours of RSM, the response can be represented graphically. For RSM, to measure the experimental data and identify the pertinent release model terms as indicated by equation 5, the second-order polynomial equation was used.

4. Statistical analysis of experimental data, and model development

The Design Expert version 11 tool was utilized to analyze the experimental data using repeated measures ANOVA and response surface regression techniques with a 5% level of significance.

RESULTS AND DISCUSSIONS

1. Responses from the adsorption capacity of crude oil onto *Sargassum latifolium*

The oil adsorption capacity of the seaweed, *S. latifolium*, was thoroughly examined. Experiments for the optimization of crude oil removal were done by varying the contact time, crude oil concentration, weight of adsorbent, and pH, and they were then correlated with responses obtained from Table (2). The response (Adsorption capacity) was estimated as related to the results of laboratory experiments by applying the BB experimental design. The output was summarized for an additional analysis of variance (ANOVA). The second-order model was adopted to assess this performance and establish the optimization process (Zaid *et al.*, 2022).

1.1. Fit summary statistics

The data and test results for all distributions used to fit the model are summarized in the fit summary. This model fits the data into first-order or linear, second-order, quadratic, and cubic equations. The highest-order polynomial models preferred from the fit summary analysis are presented in Table (3). This fit summary suggests both quadratic models with significant terms. *P*-values ≤ 0.05 suggest the significance of the model (Gharbani & Nojavan, 2017).

Table 2. Fit summary for the adsorption capacity

Source	Std. Dev.	R-Squared	Adjusted R-Squared	Predicted R-Squared	PRESS	
Linear	5.396069	0.797099	0.763283	0.688925	1071.39	
2FI	4.388279	0.899358	0.843446	0.619728	1309.717	
Quadratic	1.744538	0.987629	0.975258	0.912675	300.7613	Suggested
Cubic	1.299309	0.996079	0.986275			Aliased

1.2 Adsorption capacity model selection and analysis of variance

The results of the analysis of BB responses, and the analysis of variance for research of the ability of crude oil adsorption onto *Sargassum Latifolium* are shown in Table (3).

The use of ANOVA is essential to assess the relevance and suitability of the model. It separates the overall variance of the results into the variance of the model and the variance of the experimental error, demonstrating if the model's variation is considerable in comparison to the residual error's variation (Hemmati & Rashidi, 2019). This comparison is carried out using Fisher's F-test value, which measures the relationship between the model's mean square and the residual error (Khataee *et al.*, 2010). As presented in Table (4), the model significance is suggested by the model's F-value of 79.83. A "Model F-value" may happen only 0.01% of the time; this may happen

due to noise. Values of "Prob> F" less than 0.0500 designate that the model terms are significant. In this case, X_1 (adsorbent dose), X_2 (oil volume), X_3 (Time), X_1X_2 (adsorbent dose, oil volume), X_1X_4 (adsorbent dose, pH), X_2X_3 (oil volume, Time), X_2X_4 (oil volume, pH), X_2^2 (oil volume)², X_3^2 (Time)², and X_4^2 (pH)² were significant model terms.

Table 3. Analysis of variance (ANOVA - response surface quadratic model) for the adsorption capacity of crude oil onto *Sargassum Latifolium*

Source	Sum of squares	df	Mean square	F value	P-value	Prob > F
Model	3401.549	14	242.9678	79.83396	< 0.0001	Significant
A-adsorbent dose						
(X_1)	141.1256	1	141.1256	46.37082	< 0.0001	
B-Oil concentration						
(X_2)	984.8601	1	984.8601	323.6037	< 0.0001	
C-Time (X_3)	1.936757	1	1.936757	0.636376	0.4383	
D-pH (X_4)	279.4983	1	279.4983	91.83708	< 0.0001	
X_1X_2	102.2197	1	102.2197	33.58719	< 0.0001	
X_1X_3	1.523128	1	1.523128	0.500467	0.4909	
X_1X_4	86.21123	1	86.21123	28.32714	0.0001	
X_2X_3	48.3025	1	48.3025	15.87115	0.0014	
X_2X_4	98.98867	1	98.98867	32.52553	< 0.0001	
X_2X_4	2.031039	1	2.031039	0.667355	0.4277	
X_1^2	1.921501	1	1.921501	0.631364	0.4401	
X_2^2	128.0098	1	128.0098	42.06123	< 0.0001	
X_3^2	42.40512	1	42.40512	13.9334	0.0022	
X_4^2	144.8401	1	144.8401	47.5913	< 0.0001	
Residual	42.6078	14	3.043414			
Lack of fit	29.10216	6	4.850361	2.873088	0.0848	Not significant
Pure error	13.50564	8	1.688205			
Cor total	3444.157	28				

Using replicated design points, the "Lack of fit test" compares residual error to pure error. The P -value is >0.05 , hence the F -value of 2.87 indicates that a lack of fit is not significant. The model's non-significant lack of fit demonstrated that it was appropriate for the current work.

The resulting RSM equation (in terms of coded factors) obtained from the improved model is presented below in equation 2.

$$R1 = 20.396 - 4.20481 * X_1 + 9.703122 * X_2 - 0.5252 * X_3 + 5.681013 * X_1 * X_2 - 0.75714 * X_1 * X_3 - 4.6425 * X_1 * X_4 + 3.475 * X_2 * X_3 + 4.581325 * X_2 * X_4 - 1.11809 * X_3 * X_4 - 0.58202 * X_1^2 + 4.614176 * X_2 - 3.03346 * X_3 - 5.01476 * X_4^2 \quad (2)$$

According to R^2 , the model's determination coefficient was 0.987, which suggested that predicted values and the experimental data points fit each other well. (Fig. 1 & Table 4). Additionally, this suggests that the independent variables account for 98.7% of the changes in crude oil adsorption, proving that the model does not simply account for 1.3 percent of the variation. Predicted R^2 is a gauge of a model's accuracy in predicting a response value. To be considered reasonable agreement, the adjusted R^2 and anticipated R^2 must be within 0.20 of one another. If they aren't, there can be a problem with the model or the data. In our example, the expected R^2 of 0.912 and the adjusted R^2 of 0.975 are reasonably in agreement. To determine whether the precision is adequate, the range of the anticipated values of design points is contrasted with the average prediction error. An ideal ratio is more than 4, which implies adequate model discrimination. The ratio in this study was 29.9, demonstrating the reliability of the experiment's findings. The degree of precision is indicated by the standard deviation ($SD = 1.7$) and coefficient of variation ($CV = 8.25\%$). The experiment is conducted adequately, as evidenced by the low values of CV and SD . The models expose a high R^2 value, a substantial F -value, a negligible P -value for lack of fit, and a low variance SD . These findings explain the great accuracy of the prediction of crude oil's adsorption capacity by *S. latifolium*. Therefore, the models were used for further analysis.

Table 4. Summary of regression statistics for the adsorption capacity of crude oil onto *S. Latifolium*

Std. Dev.	1.744538	R- Squared	0.987629
Mean	21.14207	Adj R- Squared	0.975258
C.V. %	8.251503	Pred R- Squared	0.912675
PRESS	300.7613	Adeq Precision	29.95594

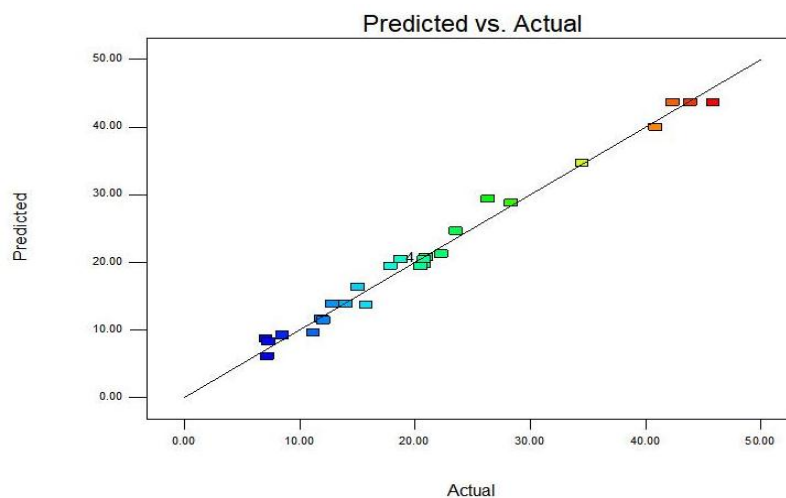


Fig. 1. Plot of the experimental and predicted responses

1.3 Interaction effect of the independent variables

Fig. (2) provides RSM plots of the second-order polynomial equation with two variables varied within predetermined experimental ranges, while the other two were held constant.

Fig. (2a, b, c) represents the RS plots of the effects of oil concentration, time, pH, and adsorbent dose on the crude oil adsorption onto *S. Latifolium*, respectively. It confirms that oil adsorption capacity decreased with increasing the initial adsorbent dose. Fig. (2c, e) shows that the response increased with increasing the initial pH. Conversely, at $\text{pH} > 10.8$, the response gradually decreased. The illustrated contours are presented in Fig. (2b, d, f) show that the response raised with raising the contact time from 10- 98, but then decreased.

Numerical optimization was applied to obtain the desired value for each input factor and response. There, the following input optimization options are available for selection: In target, range, minimum, maximum, none of the responses, and designed to produce an ideal output value under a particular set of circumstances. Under these conditions, the best results accomplished for crude oil adsorption onto *S. latifolium* was 46.14gm (Fig. 3) with an adsorbent dose of 0.13gm, oil concentration of 24.29ml, time of 57.44 minutes, and an initial pH of 9.54. The accuracy and suitability of the model were indicated by a confirmatory experiment, which revealed that the crude oil adsorption capacity onto *Sargassum latifolium* was 45.87gm under optimal conditions (actual), slightly lower than 46.14gm (predicted) obtained by the model.

2. Adsorption isotherm

Adsorption isotherm is crucial for describing how the solute and adsorbent interact and to investigate the effectiveness of adsorption as well as its mechanism. The equilibrium behavior between oil and the adsorbent has already been described using Langmuir or Freundlich isotherm models by several researchers. It was analyzed using both types of isotherms for *S. latifolium* oil adsorption. Table (5) represents the linear equations of isotherm models applied by Langmuir and Freundlich, equations 7 and 8, respectively. The values of R^2 were compared between the isotherm models with the aim to assess the validity of these models. Compared to the value derived from the Freundlich models, the R^2 values of the Langmuir model are typically significantly closer to 1, as shown in Table (6); This indicates that the Langmuir model rather than the Freundlich model best fits the experimental data. Moreover, this indicated monolayer coverage of oil on *S. latifolium*, and the adsorption occurred was chemisorption.

Table 5. List of adsorption Isotherm used

Isotherm model	Linear form equation	Reference
Langmuir	$\frac{C_e}{q_e} = \frac{1}{K_L Q_m} + \frac{C_e}{Q_m}$ <p>C_e is the equilibrium concentration of oil in liquid phase (mg/L), q_e is the equilibrium concentration of oil in the adsorbed phase, Q_m is the maximum adsorption capacity of the solute (mg/g) and K_L is an Langmuir adsorption equilibrium constant (L/mg).</p>	(Thabet et al. 2020; Abeer A. Moneer et al. 2022)
Freundlich	$\ln q_e = \ln K_F + \frac{1}{n} \ln C_e$ <p>K_F (mg/g) represents the Freundlich adsorption coefficient and (n) is the Freundlich constant.</p>	(Ashour et al. 2022)

3. *Sargassum Latifolium* characterization

3.1 FT-IR analysis

Finding functional groups that can adsorb ions of *S. latifolium* is possible with the help of FTIR spectrophotometry, which was used to elucidate these active sites. Peaks in the *S. latifolium* FTIR spectrum (Fig. 4) were attributed to distinct groups and bonds based on the wave numbers (cm^{-1}) that corresponded to each peak, which were described in the literature to be in the range of 500–4000 cm^{-1} . The band observed at 3395 cm^{-1} in *S. latifolium* represents the bonded –OH group on their surface. The light stretches at 2923, 2853, and 2729 cm^{-1} demonstrated the stretching of aliphatic acids' symmetric or asymmetric C-H vibration. Amide molecules may be responsible for the band observed at 1630 cm^{-1} , which represents C=O bond. Furthermore, ionic carboxylic groups (-COO) showed symmetric and asymmetric stretching vibrations at 1480 cm^{-1} . While adsorption band at 1376 cm^{-1} indicates C-H presence bend. In *S. latifolium*, a deformation associated with the C–O bond was noted at 1161 and 1032 cm^{-1} . The FTIR analysis revealed a band at a range of 812–871 cm^{-1} representing the Al–O–Si. In addition, the C-H bond of aromatic compounds can be credited with the peak at 725 cm^{-1} . These functional groups, which include hydroxyl, amino, carbonyl, and carboxyl, have been demonstrated to be present in a number of biomolecules, proteins, and extracellular polymers. These groups are primarily in charge of the sorption of *S. latifolium* by chemical bonding (Singaravelu et al., 2007; Azizi et al., 2014; Mansour et al., 2022). FTIR analysis suggests that the *S. latifolium* ions interaction with adsorbent active sites may be responsible for the formation of new adsorption peaks, transfer in wave number of functional groups, and adsorption strength modifications. The *S. latifolium* ions were electrostatically drawn to the active areas of the adsorbents. Moreover, the electrostatic attraction occurred between the *S. latifolium* ions and the carbonate group.

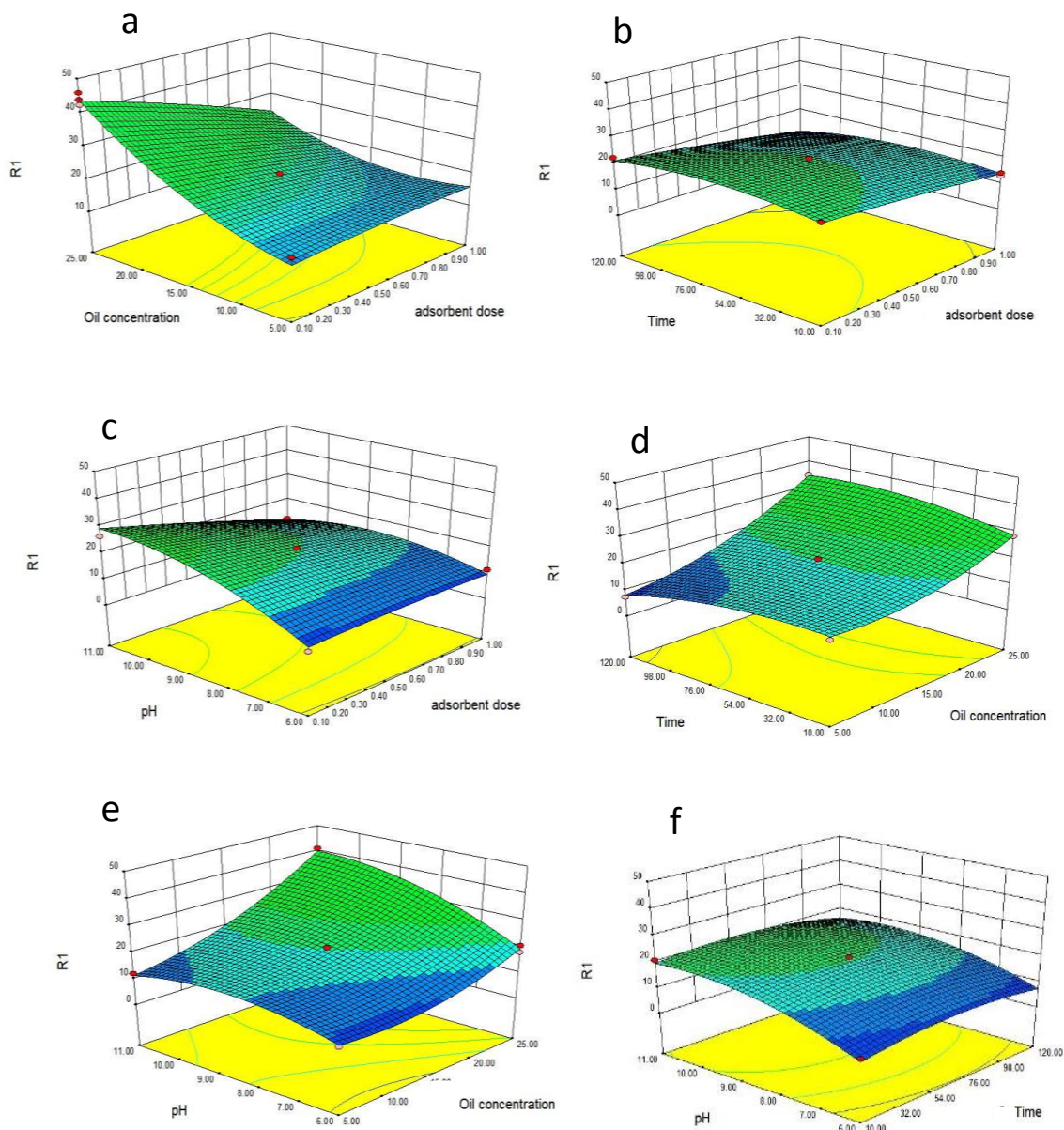


Fig. 2. Response surface plots for crude oil adsorbent capacity onto *Sargassum Latifolium* showing:

- Effect initial concentration/adsorbent dose (pH 8.5, time 65min),
- Effect time/Adsorbent dose (initial concentration 15ml, pH 8.5),
- Effect pH/ adsorbent dose (initial concentration 15ml, time 65min),
- Effect time/initial concentration (adsorbent dose 0.55gm, pH 8.5),
- Effect pH/initial concentration (adsorbent dose 0.55gm, time 65min), and
- Effect pH/ time (adsorbent dose 0.55gm, initial concentration 15ml)

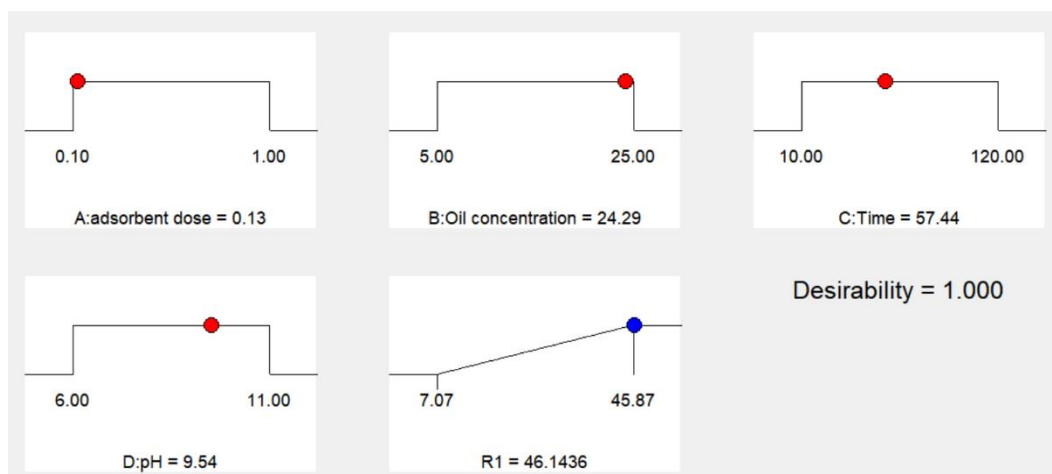


Fig. 3. Desirability ramps for optimization

Table 6. Results of isotherm models of oil adsorption onto *Sargassum latifolium*

Isotherm Model	Parameters	<i>Sargassum latifolium</i>
Langmuir	Q_m (mg/g)	20.66
	K_L (L/mg)	0.081
	R^2	0.936
Freundlich	K_f (mg/g)	26.380
	$1/n$	0.0394
	R^2	0.0570

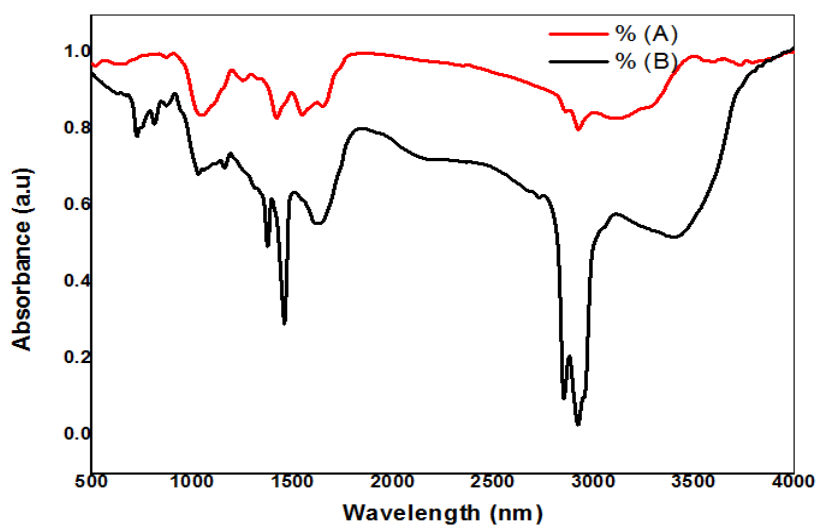


Fig. 4. FTIR spectra of (*Sargassum latifolium*) (A) Before adsorption and (B) After the process

3.2 SEM analysis

The SEM of *S. latifolium* showed that surface shape changes dramatically after adsorption, and unique aggregates form on their surfaces.

Fig. (5) illustrates the SEM images of *S. latifolium* before and after oil removal at magnification of 2,000 X. The *S. latifolium* interaction with oil resulted in the formation of flake-like deposits on its surface, causing the surface to become irregular. The *S. latifolium* had a thick and extremely porous morphology with diverse sizes and forms of surface texture, as displayed in Fig. (5). In the meantime, due to the adsorption of the *S. latifolium*, the porous texture on the surface. Following contact with oil, the swollen deposits appeared.

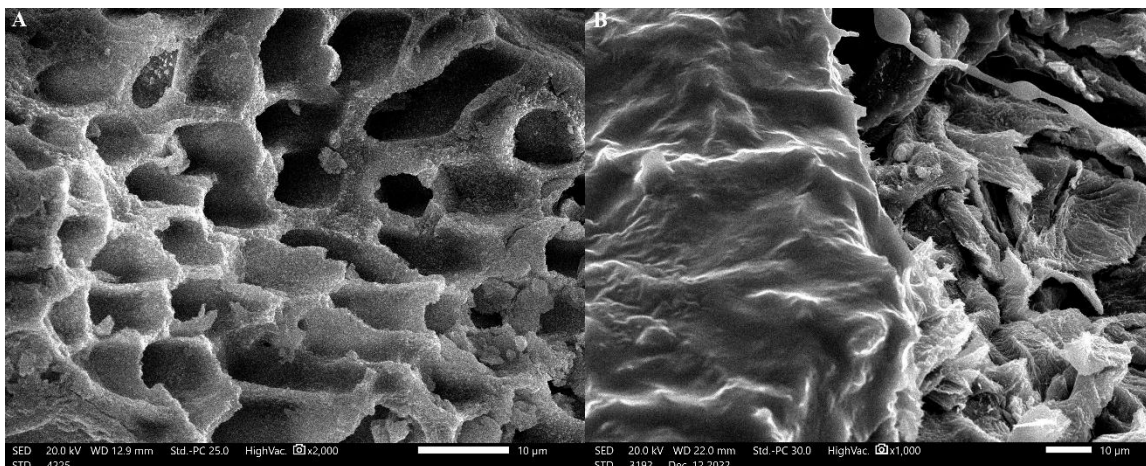


Fig. 5. SEM images of (*S. latifolium*) (A) Before adsorption and (B) After adsorption

3.3 BET characterization

To determine whether the sample's porosity had undergone any change, the adsorbent's precise pore volumes and surface area were examined., as shown in Table (7). At low pressures (P/P_0 0.01), the *S. Latifolium* isotherm exhibits rapid N_2 adsorption and constant high adsorption with hysteresis. The BET surface area is determined to be 111.65m²/ g. Pollutant trapping is crucial due to pores acting as receptor or binding sites during the adsorption. Moreover, 0.122cc/ g of pore volume is provided.

Table 7. N_2 adsorption determined the textural characteristics of *S. latifolium*

BET Single point	Surface Area (m ² /g)				Whole Pore Volume (cc/g)	Mean Pore Size (nm)	Mean Particle radius (nm)
	BET Surface area	Langmuir method	DH adsorption	DH desorption			
100.78 0	111.650	178.400	69.789	59.7729	0.122 cc/g	2.190 nm	1.220 nm

3.4 Raman spectra

The Raman spectra, as well as FT-IR, provide a definitive identification of the adsorbent particles. The dry Raman spectra of *S. latifolium* are shown in Fig. (6). The most Raman bands that confirm adsorbent success were seen around 1736- 1751, 1434-1461, 826- 878, and 634- 698 cm^{-1} . These peaks, in that sequence, matches to the vibrations of the ester C=O that stretch, the CH₃-symmetric deformation, the H₃C-C stretching, and the O-C=O in-plane deformation. The C=O stretching vibration in the aldehyde group produced an extra band at 1608 cm^{-1} . Assignable to asymmetric and symmetric C-O-C stretch modes, C-OH bending modes and the band connected to the adsorbent's C-H₂ bonds are the distinctive bands at 1094, 1265, and 1378 cm^{-1} .

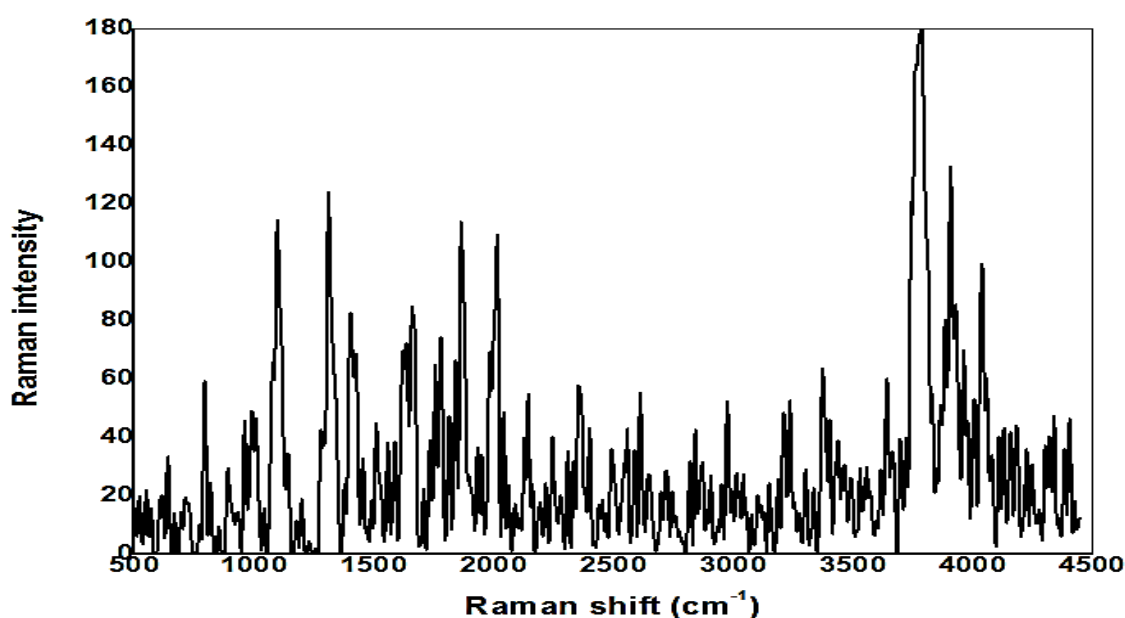


Fig. 6. Raman of *S. latifolium* adsorbent

3.5. Comparison of oil adsorption capacity *S. latifolium* with different raw and modified adsorbents

Table (8) demonstrates the comparison of the oil removal capacity *S. latifolium* with different raw and modified adsorbents. The findings exposed very effective adsorbent for oil removal capacity compared to previous studies. Most of the mentioned studies used crude oil as the type of oil removed.

The comparison between different types of adsorbents, including natural or modified adsorbents such as activated carbon, polymers, and other composites, was recorded for oil removal. The widely utilized adsorbents are recognized to be biosorbents. One of the benefits of using biosorbents is how simple it is to prepare them, along with other benefits like biodegradability and cost-effectiveness. In certain cases, the source

biomass material is only ground up, cleaned, dried, and used for adsorption tests without any kind of preparation (Emenike *et al.*, 2022). For example, black rice husk ash, date palm, modified palm fibers, modified cotton fibers, banana peel, raw nettle fibers, bagasse, raw *Posidona oceanic*, rice straw, and *S. Latifolium*, all are examples of good bioadsorbents for oil removal from aqueous solution, as indicated in Table (8).

Table 8. Comparison of oil adsorption capacity *S. Latifolium* with raw and modified adsorbents

Adsorbent	Oil capacity (g/g ⁻¹)	Type of oil	Reference
Black rice husk ash (BRHA) adsorbent	6.220; 5.020	Crude oil; Diesel oil	(Vlaev <i>et al.</i> , 2011)
Date palm	1.425	Petroleum oil	(Sueyoshi <i>et al.</i> , 2012)
Zeolite fine powder	0.192	Motor oil	(Ramezanzadeh <i>et al.</i> , 2016)
Modified palm fibers	35.710, 22.730 and 21.740	Crude oil, Diesel oil, vegetable oil	(O. Abdelwahab, Nasr & Thabet, 2017)
Modified cotton fiber	57	Diesel, Crude oil	(Lv <i>et al.</i> , 2018)
Banana peel	6.630	Crude oil	(Alaa El-Din <i>et al.</i> , 2018)
Raw nettle fibres	8.320	Crude and diesel engine oil	(Viju <i>et al.</i> , 2019)
Acetylated nettle fibres	18.800	Crude oil and diesel engine oil	(Viju <i>et al.</i> , 2019)
Raw <i>Posidona oceanic</i>	5.320	Crude oil	(Ben Jmaa & Kallel, 2019)
Activated carbon nanofiber nonwoven	1.250	Crude oil	(Waisi <i>et al.</i> , 2020)
Polymeric adsorbent beads	0.300	Crude oil	(Al-Maas <i>et al.</i> , 2022)
Chitosan	32.200	Crude oil	(Khalifa <i>et al.</i> , 2019)
Nonanyl chitosan Schiff base	59.200	Crude oil	(Khalifa <i>et al.</i> , 2019)
Chitosan-g-poly (butyl acrylate)	83.300	Crude oil	(Omer <i>et al.</i> , 2020)
Rice straw	6.670	Crude oil	(Tayeb <i>et al.</i> , 2020)
Carbonaceous nano-sponge	33	Crude oil	(Torasso <i>et al.</i> , 2019)
Silver nanoparticle	2.660	Crude oil	(Akpomie & Conradie, 2021)
Nano-magnetic/activated carbon	30.200	Crude oil	(Shokry, Elkady & Salama, 2020)
<i>Sargassum Latifolium</i>	45.870	Crude oil	Present study

In a common modification process called acetylation (acetylated nettle fibers), some of the hydrophilic hydroxyl (-OH) groups in lignocellulosic materials are swapped out for the hydrophobic acetyl (-COCH₃) groups, therefore acetylated nettle fibers were effective with oil removal of 18.8g/ g oil (Viju *et al.*, 2019).

Some researchers investigated the activated carbon for oil removal due to its mesoporous structure, high hydrophobicity, and high specific surface area. Waisi *et al.* (2020) studied crude oil adsorption using activated carbon derived from nanofiber nonwoven, with a removal capacity of 1.25g oil/ g adsorbent.

Others used polymers due to their unique qualities, including their low cost, biodegradability, biocompatibility, tunable surface chemistry, and mechanical stiffness, such as chitosan and chitosan-modified adsorbent with high oil adsorption and retention capacities, excellent oil-water selectivity, and high reusability (Khalifa *et al.*, 2019; Omer *et al.*, 2020).

Nanoparticles from organic and inorganic sources have been used for crude oil removal from water. Torasso *et al.* (2019) developed a superhydrophobic and oleophilic carbonaceous nanosponge to specifically oil removal with a capacity of 33g oil/ g adsorbent. The light crude oil may be absorbed 33 times its own weight by the nano-adsorbent, with little water adsorption. The utilization of a silver nanoparticle for oil removal from oily wastewater was addressed in the study of Akpomie and Conradie (2021). Other researchers used two or more constituents in a material called composite, a combination of different kinds of adsorbents to improve the adsorbent prosperities; nevertheless, not many researchers studied this kind of adsorbent (Shokry, Elkady & Salama, 2020; Emenike *et al.*, 2022). While, in the present study, *S. latifolium* was used for crude oil removal and found to be very effective with a high removal capacity of 45.87g/ g oil. Additionally, natural biosorbents offer additional benefits due to their ease of preparation, as previously indicated..

CONCLUSION

The present study investigates the oil adsorption onto *S. latifolium*. Four independent variables were experimentally applied including adsorbent dosage, oil volume, contact time, and pH. Response surface methodology developed the Box-Behnken model for the examination of the role of these parameters on oil removal. The average pore size of the adsorbent was 2.190nm as determined by BET measurements. Additionally, the surface area analysis (BET) of Brunauer-Emmett-Teller was proven to be 0.00351m²/ g. Furthermore, a SEM showed that the interaction of *Sargassum latifolium* with oil led to the development of flake-like deposits on its surface, causing the surface to become uneven. The principal functional groups engaged in the treatment process were carboxyl, hydroxyl, amine, and carbonyl, according to the FTIR spectrum. The best results accomplished for crude oil adsorption were obtained at the optimum conditions of adsorbent dose of 0.13gm, oil concentration of 24.29ml, time of 57.44

minutes, and initial pH of 9.54. The confirmatory experiment demonstrated the model's applicability and accuracy, which revealed that the crude oil adsorption capacity onto *Sargassum latifolium* was 45.87gm under optimal conditions, slightly lower than 46.14gm (predicted) obtained by the model. For isotherm models, the Langmuir model rather than the Freundlich model better fits the experimental data, indicating monolayer coverage and a chemisorption adsorption process. According to the results, *Sargassum latifolium* showed an excellent oil uptake and indicated to be a great choice as a bioadsorbent for oil removal from aqueous environments.

REFERENCES

Abd El-Hamid, H. T.; AlProl, A. E. and Hafiz, M. A. (2022). The Efficiency of Adsorption Modelling and Plackett-Burman Design for Remediation of Crystal Violet by *Sargassum Latifolium*. *Biocatal. Agric. Biotechnol.*, 44 (September): 102459. <https://doi.org/10.1016/j.bcab.2022.102459>.

Abdelwahab, O.; Samir, M. N. and Walaa, M. T. (2017). Palm Fibers and Modified Palm Fibers Adsorbents for Different Oils. *Alexandria Eng. J.*, 56 (4): 749–55. <https://doi.org/10.1016/j.aej.2016.11.020>.

Abdelwahab, O. E.; Nasr S. M.; and Thabet W. M.; (2021) “Oil spill cleanup using modified modified Palm fibers: Trial for practical application”, *Egyptian Journal of Aquatic Biology & Fisheries*. Volume. 25. Issue.2 .pp: 457-464.

Abdelwahab, O. and Thabet, W. M. (2023). Natural Zeolites and Zeolite Composites for Heavy Metal Removal from Contaminated Water and Their Applications in Aquaculture Systems: A Review. *Egypt. J. Aquat. Res.*, National Institute of Oceanography and Fisheries. <https://doi.org/10.1016/j.ejar.2023.11.004>.

Abuhasel, K.; Mohamed, K.; Mohammed, A.; Yamuna, M. and Yong, T. J. (2021). Oily Wastewater Treatment: Overview of Conventional and Modern Methods, Challenges, and Future Opportunities. *Water*, 13 (7): 980. <https://doi.org/10.3390/w13070980>.

Adetunji, A. I. and Ademola, O. O. (2021). Treatment of Industrial Oily Wastewater by Advanced Technologies: A Review. *Appl. Water Sci.*, 11 (6): 98. <https://doi.org/10.1007/s13201-021-01430-4>.

Akpomie, K. G. and Jeanet, C. (2021). Ultrasonic Aided Sorption of Oil from Oil-in-Water Emulsion onto Oleophilic Natural Organic-Silver Nanocomposite. *Chem. Eng. Res. Des.*, 165 (January): 12–24. <https://doi.org/10.1016/j.cherd.2020.10.019>.

Alaa El-Din, G.; Amer, A.A.; Malsh, G. and Hussein, M. (2018). Study on the Use of Banana Peels for Oil Spill Removal. *Alexandria Eng. J.*, 57 (3): 2061–68. <https://doi.org/10.1016/j.aej.2017.05.020>.

Ale, M. T.; Jørn, D. M. and Anne, S. M. (2011). Important Determinants for Fucoidan Bioactivity: A Critical Review of Structure-Function Relations and Extraction Methods for Fucose-Containing Sulfated Polysaccharides from Brown Seaweeds. *Mar. Drugs*, 9 (10): 2106–30. <https://doi.org/10.3390/md9102106>.

Al-Maas, M.; Joel, M.; Igor, K.; Mariam, A. A. and Samer, A. (2022). Evaluation of Polymeric Adsorbents via Fixed-Bed Columns for Emulsified Oil Removal from Industrial Wastewater. *J. Water Process Eng.*, 49 (October): 102962. <https://doi.org/10.1016/j.jwpe.2022.102962>.

Alprol, A. E.; Khedawy, M.; Ashour, M. and Walaa, M. T. (2023). *Arthrospira Platensis* Nanoparticle-Based Approach for Efficient Removal of Methyl Orange Dye from Aqueous Solutions: Isotherm, Kinetic, and Thermodynamic Analysis. *Biomass Convers. Biorefin.*, October. <https://doi.org/10.1007/s13399-023-04844-z>.

Ashour, M.; Alprol, A. E.; Khedawy, M.; Abualnaja, K. M. and Mansour, A. T. (2022). Equilibrium and Kinetic Modeling of Crystal Violet Dye Adsorption by a Marine Diatom, *Skeletonema Costatum*. *Materials*, 15 (18): 6375. <https://doi.org/10.3390/ma15186375>.

Azizi, S.; Mansor, B. A.; Farideh, N. and Rosfarizan, M. (2014). Green Biosynthesis and Characterization of Zinc Oxide Nanoparticles Using Brown Marine Macroalga *Sargassum Muticum* Aqueous Extract. *Mater. Lett.*, 116 (February): 275–77. <https://doi.org/10.1016/j.matlet.2013.11.038>.

Demirel, C.; Abraham, K.; David, H.; Aleš, S.; Čestmír, M. and Oldřich, D. (2022). Using Box–Behnken Design Coupled with Response Surface Methodology for Optimizing Rapeseed Oil Expression Parameters under Heating and Freezing Conditions. *Processes*, 10 (3): 490. <https://doi.org/10.3390/pr10030490>.

Diraki, A.; Hamish, R. M.; Gordon, M. and Ahmed, A. (2022). Removal and Recovery of Dissolved Oil from High-Salinity Wastewater Using Graphene–Iron Oxide Nanocomposites. *Applied Sciences*, 12 (19): 9414. <https://doi.org/10.3390/app12199414>.

Emenike, E. C.; Joy, A.; Kingsley, O. I.; Samuel, O.; Comfort, A. A.; Victor, T. A.; Hussein K. O. and Adewale, G. A. (2022). Adsorption of Crude Oil from Aqueous Solution: A Review. *J. Water Process Eng.*, 50 (December): 103330. <https://doi.org/10.1016/j.jwpe.2022.103330>.

Gharbani, P. and Azam, N. (2017). Response Surface Methodology for Optimizing Adsorption Process Parameters of Reactive Blue 21 onto Modified Kaolin. *Advances in Environmental Technology*, 3 (2): 89–98. <https://doi.org/10.22104/aet.2017.505>.

Ghoneim, M. M.; Hanaa, S. E.; Khalid, M. E., Adel, A.; Emad, H. A.; Lamiaa, I. M. and Al-prol, A. E. (2014). Removal of Cadmium from Aqueous Solution Using Marine Green Algae , *Ulva Lactuca*. *The Egyptian Journal of Aquatic Research*, 40 (3): 235–42. <https://doi.org/10.1016/j.ejar.2014.08.005>.

Gomaa, M.; Mustafa, A. F.; Awatief, F. H. and Khayria, M. A. (2018). Use of the Brown Seaweed *Sargassum Latifolium* in the Design of Alginate-Fucoidan Based Films with Natural Antioxidant Properties and Kinetic Modeling of Moisture Sorption and Polyphenolic Release. *Food Hydrocolloids*, 82 (September): 64–72. <https://doi.org/10.1016/j.foodhyd.2018.03.053>.

Han, M.; Jin, Z.; Wen, C.; Jiahao, C. and Gongfu, Z. (2019). Research Progress and Prospects of Marine Oily Wastewater Treatment: A Review. *Water* 11 (12): 2517. <https://doi.org/10.3390/w11122517>.

Hemmati, A. and Hamed, R. (2019). Optimization of Industrial Intercooled Post-Combustion CO₂ Absorber by Applying Rate- Base Model and Response Surface Methodology (RSM). *Process Safety and Environmental Protection*, 121 (January): 77–86. <https://doi.org/10.1016/j.psep.2018.10.009>.

Jmaa, S. B. and Amjad, K. (2019). Assessment of Performance of *Posidona Oceanica* (L.) as Biosorbent for Crude Oil-Spill Cleanup in Seawater. *Biomed Res. Int.* 2019 (October): 1–9. <https://doi.org/10.1155/2019/6029654>.

Khalifa, R. E.; Omer, A.M.; Tamer, T. M.; Ali, A.A; Ammar, T.A. and Mohy Eldin, M. S. (2019). Efficient Eco-Friendly Crude Oil Adsorptive Chitosan Derivatives: Kinetics, Equilibrium and Thermodynamic Studies. *Desalin. Water Treat.*, 159: 269–81. <https://doi.org/10.5004/dwt.2019.24166>.

Khataee, A. R.; Fathinia, M.; Aber, S. and Zarei, M. (2010). Optimization of Photocatalytic Treatment of Dye Solution on Supported TiO₂ Nanoparticles by Central Composite Design: Intermediates Identification. *J. Hazard. Mater.*, 181 (1–3): 886–97. <https://doi.org/10.1016/j.jhazmat.2010.05.096>.

Lee, X. J.; Hwai, C. O.; Jecksin, O.; Kai, L. Y.; Thing, C. T.; Wei-Hsin, C. and Yong, S. O. (2022). Engineered Macroalgal and Microalgal Adsorbents: Synthesis Routes and Adsorptive Performance on Hazardous Water Contaminants. *J. Hazard. Mater.*, 423 (February): 126921. <https://doi.org/10.1016/j.jhazmat.2021.126921>.

Lv, N.; Xiaoli, W.; Shitao, P.; Lei, L. and Ran, Z. (2018). Superhydrophobic/Superoleophilic Cotton-Oil Absorbent: Preparation and Its Application in Oil/Water Separation. *RSC Advances*, 8 (53): 30257–64. <https://doi.org/10.1039/C8RA05420G>.

Mansour, A. T.; Alprol, A. E.; Abualnaja, K. M.; El-Beltagi, H. S.; Ramadan, K. M. A. and Ashour, M. (2022). Dried Brown Seaweed's Phytoremediation Potential for Methylene Blue Dye Removal from Aquatic Environments. *Polymers*, 14 (7): 1375. <https://doi.org/10.3390/polym14071375>.

Medeiros, A. D. M.; Cláudio, J. G. S. J.; Julia, D. P. A.; Italo, J. B. D.; Andréa, F. S. C. and Leonie, A. S. (2022). Oily Wastewater Treatment: Methods, Challenges, and Trends. *Processes*, 10 (4): 743. <https://doi.org/10.3390/pr10040743>.

Moneer, A. A.; Thabet W.M.; Khedawy, M.; El-Sadaawy, M. M. and Shaaban, N. A. (2023). Electrocoagulation Process for Oily Wastewater Treatment and Optimization Using Response Surface Methodology. *Int. J. Environ. Sci. Technol.*, June. <https://doi.org/10.1007/s13762-023-05003-7>.

Moneer, A. A.; El-Mallah, N. M.; El-Sadaawy, M. M.; Khedawy, M. and Ramadan, M. S.H. (2022). Parameters Optimization, Kinetics, Isotherm Modeling of Cationic and Disperse Dyes Removal Procedure Using Bi-Polar Iron Electrocoagulation System. *Desalin. Water Treat.*, 256: 300–313. <https://doi.org/10.5004/dwt.2022.28416>.

Omer, A. M.; Randa, E. K.; Tamer, M. T.; Ahmed, A. A.; Yossry, A. A. and Mohamed, S. M. (2020). Kinetic and Thermodynamic Studies for the Sorptive Removal of Crude Oil Spills Using a Low-Cost Chitosan-Poly (Butyl Acrylate) Grafted Copolymer. *Desalin. Water Treat.*, 192: 213–25. <https://doi.org/10.5004/dwt.2020.25704>.

Prol, A. E.; El-Metwally, M. E. A. and Amer, A. (2019). *Sargassum Latifolium* as Eco-Friendly Materials for Treatment of Toxic Nickel (II) and Lead (II) Ions from Aqueous Solution. *Egypt. J. Aquat. Biol. Fish.*, 23 (5Special Issue): 285–99. <https://doi.org/10.21608/ejabf.2019.66839>.

Putatunda, S. S.; Bhattacharya, D. S. and Bhattacharjee, C. (2019). A Review on the Application of Different Treatment Processes for Emulsified Oily Wastewater. *Int. J. Environ. Sci. Technol.*, 16 (5): 2525–36. <https://doi.org/10.1007/s13762-018-2055-6>.

Ramezanzadeh, B. S.; Niroumandrad, A. A.; Mahdavian, M. and Moghadam. M. H. M. (2016). Enhancement of Barrier and Corrosion Protection Performance of an Epoxy Coating through Wet Transfer of Amino Functionalized Graphene Oxide. *Corros. Sci.* 103 (February): 283–304. <https://doi.org/10.1016/j.corsci.2015.11.033>.

Shokry, H.; Marwa, E. and Eslam S. (2020). Eco-Friendly Magnetic Activated Carbon Nano-Hybrid for Facile Oil Spills Separation. *Sci. Rep.*, 10 (1): 10265. <https://doi.org/10.1038/s41598-020-67231-y>.

Singaravelu, G.; Arockiamary, J. S.; Ganesh, K. V. and Govindaraju, K. (2007). A Novel Extracellular Synthesis of Monodisperse Gold Nanoparticles Using Marine Alga, *Sargassum Wightii* Gréville. *Colloids Surf., B.*, 57 (1): 97–101. <https://doi.org/10.1016/j.colsurfb.2007.01.010>.

Sueyoshi, M.; Rashid, S. A.; Baba, J.; Masaharu, T.; Kazuo, O.; Hitoshi, K.; Hidenori, Y.; Kunimasa, S. and Yu, H. (2012). Preparation and Characterization of Adsorbents for Treatment of Water Associated with Oil Production. *J. Anal. Appl. Pyrolysis.*, 97 (September): 80–87. <https://doi.org/10.1016/j.jaap.2012.04.003>.

Tayeb, A. M.; Rania, F.; Olfat, A. M. and Maha, A. T. (2020). Oil Spill Clean-up Using Combined Sorbents: A Comparative Investigation and Design Aspects. *Int. J. Environ. Anal. Chem.*, 100 (3): 311–23. <https://doi.org/10.1080/03067319.2019.1636976>.

Thabet, W.; Somia, A.; Abdelwahab, O. and Soliman, N. (2020). Enhancement Adsorption of Lead and Cadmium Ions from Waste Solutions Using Chemically Modified Palm Fibers. *Egypt. J. Chem.*, 63 (12): 4917-4927. <https://doi.org/10.21608/ejchem.2020.31220.2663>.

Soliman, N., Thabet, W.M., El-Sadaawy, M.M., Morsy, F.A.M., (2022) Contamination Status and Potential Risk of Metals in Marine Sediments of Shalateen Coast, the Red Sea. *Soil and Sediment Contamination: An International Journal*, 31, 40–56. <https://doi.org/10.1080/15320383.2021.1903832>.

Torasso, N.; Federico, T.; Andrés, A. D.; Norma, D.; Diana, G. and Silvia, G. (2019). Superhydrophobic Plasma Polymerized Nanosponge with High Oil Sorption Capacity. *Plasma Processes Polym.*, 16 (3). <https://doi.org/10.1002/ppap.201800158>.

Viju, S. G.; Thilagavathi, B. V. and Brindha, R. (2019). Oil Sorption Behavior of Acetylated Nettle Fiber. *The Journal of The Textile Institute*, 110 (10): 1415–23. <https://doi.org/10.1080/00405000.2019.1603184>.

Vlaev, L.; Petkov, P.; Dimitrov, A. and Genieva, S. (2011). Cleanup of Water Polluted with Crude Oil or Diesel Fuel Using Rice Husks Ash. *J. Taiwan Inst. Chem. Eng.*, 42 (6): 957–64. <https://doi.org/10.1016/j.jtice.2011.04.004>.

Waisi, B. I.; Jason, T. A.; Nieck, E. B.; Arian, N. and McCutcheon, J. R. (2020). Activated Carbon Nanofiber Nonwoven for Removal of Emulsified Oil from Water. *Microporous Mesoporous Mater.*, 296 (April): 109966. <https://doi.org/10.1016/j.micromeso.2019.109966>.

Zaid, H.; Zainab, A.; Mohammed, H. H. and Salih, R. (2022). OPTIMIZATION OF DIFFERENT CHEMICAL PROCESSES USING RESPONSE SURFACE METHODOLOGY- A REVIEW. *Journal of Engineering and Sustainable Development*, 26 (6): 1–12. <https://doi.org/10.31272/jeasd.26.6.1>.